ArvinMed Inernational

Advances in Petroleum and Chemical Engineering

APCE

Research Article

Alkhidir KEME. Arch Petro Chem Eng: APCE-101.

Electric potential gradient fractal dimension for characterizing Shajara Reservoirs of the Permo-carboniferous Shajara formation, Saudi Arabia

Khalid Elyas Mohamed Elameen Alkhidir*

Department of Petroleum and Natural Gas Engineering, college of Engineering, King Saud University, Riyadh, Saudi arabia.

***Corresponding author:** Khalid Elyas Mohamed Elameen Alkhidir, Department of Petroleum and Natural Gas Engineering, college of Engineering, King Saud University, Riyadh, Saudi Arabia. Tel: +966114679118; Email: kalkhidir@ksu.edu.sa

Citation: Alkhidir KEME (2018) Electric potential gradient fractal dimension for characterizing Shajara Reservoirs of the Permo-carboniferous Shajara formation, Saudi Arabia. Arch Petro Chem Eng: JPCE-101.

Received Date: 25 May, 2018; **Accepted Date:** 28 May, 2018; **Published Date:** 06 June, 2018

Abstract

The quality and assessment of a reservoir can be documented in details by the application of electric potential gradient. This research aims to calculate fractal dimension from the relationship among electric potential gradient, maximum electric potential gradient and wetting phase saturation and to confirm it by the fractal dimension derived from the relationship among capillary pressure and wetting phase saturation. In this research, porosity was measured on real collected sandstone samples and permeability was calculated theoretically from capillary pressure profile measured by mercury intrusion contaminating the pores of sandstone samples in consideration. Two equations for calculating the fractal dimensions have been employed. The first one describes the functional relationship between wetting phase saturation, electric potential gradient, maximum electric potential gradient and fractal dimension. The second equation implies to the wetting phase saturation as a function of capillary pressure and the fractal dimension. Two procedures for obtaining the fractal dimension have been utilized. The first procedure was done by plotting the logarithm of the ratio between electric potential gradient and maximum electric potential gradient versus logarithm wetting phase saturation. The slope of the first procedure = 3- Df (fractal dimension). The second procedure for obtaining the fractal dimension was concluded by plotting the logarithm of capillary pressure versus the logarithm of wetting phase saturation. The slope of the second procedure = Df -3. On the basis of the obtained results of the fabricated stratigraphic column and the attained values of the fractal dimension, the sandstones of the Shajara reservoirs of the Shajara Formation were divided here into three units. The gained units from bottom to top are: Lower Shajara Electric Potential Gradient Fractal Dimension Unit, Middle Shajara Electric Potential Gradient Fractal dimension Unit, and Upper Shajara Electric Potential Gradient Fractal Dimension Unit. The results show similarity between electrical potential gradient fractal dimension and capillary pressure fractal dimension. It was also noted that samples with wide range of pore radius were characterized by high values of fractal dimensions due to an increase in their connectivities. In our case, and as conclusions the higher the fractal dimension, the higher the heterogeneity, the higher the permeability, the better the reservoir characteristics.

Keywords: Capillary pressure fractal dimension; Electric potential gradient fractal dimension; Shajara Formation; Shajara Reservoirs.

Introduction

The wetting phase saturation can be described as function of capillary pressure and fractal dimension was demonstrated by [1]. The Purcell model was found to be the best fit to the experimental data of the wetting phase relative permeability for the cases as long as the measured capillary pressure curve had the same residual saturation as the relative permeability curve was described by [2]. A theoretical model to correlate capillary pressure and resistivity index based on the fractal scaling theory was reported by [3]. The fractal dimension resulting from longer transverse NMR relaxation times and lower capillary pressure reflects the volume dimension of larger pores was described by [4]. The fractal dimension derived from the short NMR relaxation times is similar to the fractal dimension of the internal surface was described by [4]. The fractal dimensions can be used to represent the complexity degree and heterogeneity of pore structure, and the coexistence of dissolution pores and large intergranular pores of Donghetang sandstones contributes to a heterogeneous pore throat distribution and a high

value of fractal dimension was reported by [5].The relationship among capillary pressure (PC), nuclear magnetic transverse relaxation time (T2) and resistivity index (I) was studied by [6]. An increase of bubble pressure fractal dimension and pressure head fractal dimension and decreasing pore size distribution index and fitting parameters m*n due to possibility of having

Materials and Methods

Sandstone samples were collected from the surface type section of the Permo-Carboniferous Shajara Formation, latitude 2652 17.4, longitude 43 36 18. (Figure1). Porosity was measured on collected samples using mercury intrusion Porosimetry and permeability was derived from capillary pressure data. The purpose of this paper is to obtain electric potential gradient fractal dimension and to confirm it by capillary pressure fractal dimension. The fractal dimension of the first procedure is determined from the positive slope of the plot of logarithm of the ratio of electric potential gradient to maximum electric potential gradient (log(II0.5/IIImax0.5) versus log wetting phase saturation (logI). Whereas the fractal dimension of the second procedure is determined from the negative slope of the plot of logarithm of log capillary pressure (log (IX) versus logarithm of wetting phase saturation (log I). The electric potential gradient can be scaled as

$$\mathbf{I} = \left[\frac{[\mathbf{II}]^{0.5}}{[\mathbf{III}]^{0.5}_{\mathbf{max}}}\right]^{\mathbf{3-Df}} \quad (\mathbf{1})$$

Where I the water saturation, II the electric potential gradient (volt/meter), $[III]_{max}$ the maximum electric potential gradient (volt/meter), and Df the fractal dimension.
Equation 1 can be proofed from

$$\mathbf{IV} = \left[\left[\frac{\mathbf{V}}{\mathbf{VI_{max}}}\right]^{2} * \mathbf{VII} * \mathbf{II}\right] \quad (\mathbf{2})$$

Where IV the electric current density in ampre/square meter, V the pore radius in meter, VI_{max} the maximum pore radius in meter, VII the electric conductivity in Siemens per meter, and II the electric potential gradient in volt per meter.
Multiply both sides of equation 2 by VI^2_{max}

$$\mathbf{IV} * \mathbf{VI^2_{max}} = [\mathbf{V^2} * \mathbf{VII} * \mathbf{II}] \quad (\mathbf{3})$$

Take the square root of equation 3

$$\sqrt{\mathbf{IV} * \mathbf{VI^2_{max}}} = \sqrt{[\mathbf{V^2} * \mathbf{VII} * \mathbf{II}]} \quad (\mathbf{4})$$

$$\mathbf{IV^{0.5}} * \mathbf{VI_{max}} = \mathbf{V} * \mathbf{VII^{0.5}} * \mathbf{II^{0.5}} \quad (\mathbf{5})$$

Rearrange equation 5

$$\mathbf{V} = \frac{\mathbf{IV^{0.5}} * \mathbf{VI_{max}}}{\mathbf{VII^{0.5}} * \mathbf{II^{0.5}}} \quad (\mathbf{6})$$

interconnected channels was confirmed by[7]. An increase of fractal dimension with increasing arithmetic, geometric relaxation time of induced polarization, permeability and grain size was investigated by [8,9,10]. An increase of seismo electric and resistivity fractal dimensions with increasing permeability and grain size was described by [11,12].
The maximum electric current density ($VIII_{max}$) can be scaled as

$$\mathbf{VI_{max}} = \frac{\mathbf{VIII^{0.5}_{max}} * \mathbf{VI_{max}}}{\mathbf{VII^{0.5}} * \mathbf{II^{0.5}}} \quad (\mathbf{7})$$

Divide equation 6 by equation 7

$$\frac{\mathbf{V}}{\mathbf{VI_{max}}} = \frac{\frac{\mathbf{IV^{0.5}} * \mathbf{VI_{max}}}{\mathbf{VII^{0.5}} * \mathbf{II^{0.5}}}}{\frac{\mathbf{VIII^{0.5}_{max}} * \mathbf{VI_{max}}}{\mathbf{VII^{0.5}} * \mathbf{II^{0.5}}}} \quad (\mathbf{8})$$

Equation 8 after simplification will become

$$\frac{\mathbf{V}}{\mathbf{VI_{max}}} = \frac{\mathbf{IV^{0.5}}}{\mathbf{VIII^{0.5}_{max}}} \quad (\mathbf{9})$$

Take the logarithm of equation 9

$$\mathbf{log}\left[\frac{\mathbf{V}}{\mathbf{VI_{max}}}\right] = \mathbf{log}\left[\frac{\mathbf{IV^{0.5}}}{\mathbf{VIII^{0.5}_{max}}}\right] \quad (\mathbf{10})$$

$$\mathbf{But;}\ \mathbf{log}\left[\frac{\mathbf{V}}{\mathbf{VI_{max}}}\right] = \frac{\mathbf{log\, I}}{\mathbf{3 - Df}} \quad (\mathbf{11})$$

Insert equation 11 into equation 10

$$\frac{\mathbf{log\, I}}{\mathbf{3 - Df}} = \mathbf{log}\left[\frac{\mathbf{IV^{0.5}}}{\mathbf{VIII^{0.5}_{max}}}\right] \quad (\mathbf{12})$$

Equation 12 after log removal will become

$$\mathbf{I} = \left[\frac{\mathbf{IV^{0.5}}}{\mathbf{VIII^{0.5}_{max}}}\right]^{\mathbf{3-Df}} \quad (\mathbf{13})$$

Equation 13 relates water saturation I; electric current density IV ; maximum electric current density $VIII_{max}$; and the fractal dimension Df
Insert equation 13 into equation 1

$$\mathbf{I} = \left[\frac{\mathbf{IV^{0.5}}}{\mathbf{VIII^{0.5}_{max}}}\right]^{\mathbf{3-Df}} = \left[\frac{[\mathbf{II}]^{0.5}}{[\mathbf{III}]^{0.5}_{\mathbf{max}}}\right]^{[\mathbf{3-Df}]} \quad (\mathbf{14})$$

Equation 14 the proof of equation 1 which relates the water saturation I, the electric potential gradient II, the maximum electric potential $(III)_{max}$ gradient, and the fractal dimension Df.
The capillary can be scaled as

$$\mathbf{log\, I} = [\mathbf{Df - 3}] * \mathbf{log\, IX} + \mathbf{constant} \quad (\mathbf{15})$$

Where I, the water saturation, IX, the capillary pressure and Df the fractal dimension.

Result and Discussion

Based on field observation the Shajara Reservoirs of the Shajara Formation of the Permo-Carboniferous Unayzah Group were divided here into three units as described in Figure1.These units from bottom to top are: Lower Shajara Reservoir, Middle Shajara reservoir, and Upper Shajara Reservoir.

Their acquired results of the electric potential gradient fractal dimension and capillary pressure fractal dimension are displayed in Table 1. Based on the attained results it was found that the electric potential gradient fractal dimension is equal to the capillary pressure fractal dimension. The maximum value of the fractal dimension was found to be 2.7872 assigned to sample SJ13 from the Upper Shajara Reservoir as verified in Table 1. Whereas the minimum value of the fractal dimension 2.4379 was reported from sample SJ3 from the Lower Shajara reservoir as displayed in Table1. The electric potential gradient fractal dimension and capillary pressure fractal dimension were observed to increase with increasing permeability as proofed in Table1 owing to the possibility of having interconnected channels.

The Lower Shajara reservoir was denoted by six sandstone samples (Figure 1), four of which label as SJ1, SJ2, SJ3 and SJ4 were selected for capillary pressure measurement as confirmed in Table1. Their positive slopes of the first procedure (log of the ratio of electric potential gradient to maximum electric potential gradient versus log wetting phase saturation) and negative slopes of the second procedure (log capillary pressure versus log wetting phase saturation (I) are delineated in Figure 2, Figure 3, Figure 4, and Figure 5. Their electric potential gradient fractal dimension and capillary pressure fractal dimension values are shown in Table 1. As we proceed from sample SJ2 to SJ3 a pronounced reduction in permeability due to compaction was reported from 1955 md to 56 md which reflects decrease in electric potential gradient fractal dimension from 2.7748 to 2.4379 as specified in table 1. Again, an increase in grain size and permeability was verified from sample SJ4 whose electric potential gradient fractal dimension and capillary pressure fractal dimension was found to be 2.6843 as described in table 1.

In contrast, the Middle Shajara reservoir which is separated from the Lower Shajara reservoir by an unconformity surface as shown in Figure 1. It was designated by four samples (Figure 1), three of which named as SJ7, SJ8, and SJ9 as illustrated in Table1 were selected for capillary measurements as described in Table 1. Their positive slopes of the first procedure and negative slopes of the second procedure are shown in Figure 6, Figure 7 and Figure 8. Additionally, their electrical potential gradient fractal dimensions and capillary pressure fractal dimensions show similarities as delineated in Table 1.Their fractal dimensions are higher than those of samples SJ3 and SJ4 from the Lower Shajara Reservoir due to an increase in their permeability as explained in table 1.

On the other hand, the Upper Shajara reservoiris separated from the Middle Shajara reservoir by yellow green mudstone as revealed in Figure 1. It is defined by three samples so called SJ11, SJ12, SJ13 as explained in Table 1. Their positive slopes of the first procedure and negative slopes of the second procedure are displayed in Figure 9, Figure 10 and Figure 11. Moreover, their electric potential gradient fractal dimension and capillary pressure fractal dimension are also higher thanthose of sample SJ3 and SJ4 from the Lower Shajara Reservoir due to an increase in their permeability as clarified in table 1.

Overall a plot of electric potential gradient fractal dimension versus capillary pressure fractal dimension as shown in Figure 12 reveals three permeable zones of varying Petrophysical properties. Such variation in fractal dimension can account for heterogeneity which is a key parameter in reservoir quality assessment. This reservoir heterogeneity was also confirmed by plotting positive slope of the first procedure versus negative slope of the second procedure as described in Figure 13.

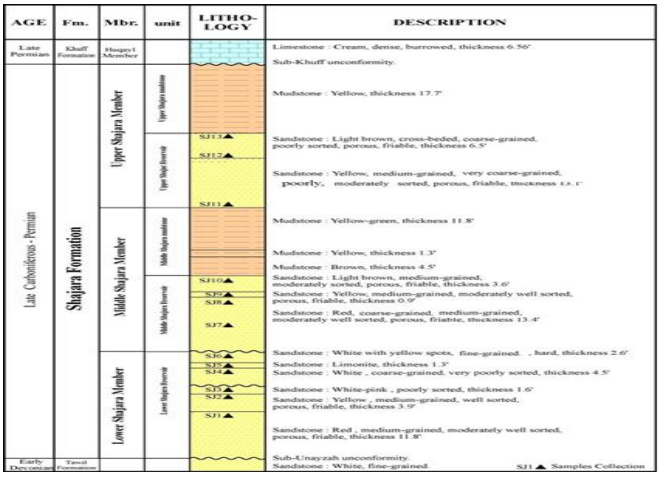

Figure 1: Stratigraphic column of the surface type section of the Permo-carboniferous Shajara Formation, latitude 2652 17.4, longitude 4336 18.

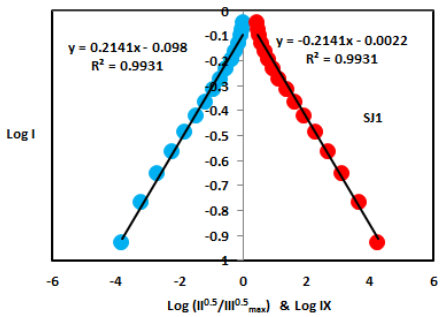

Figure 2: Log ($II^{0.5}/III_{max}^{0.5}$) versus log I (blue color)& Log IX versus log I (red color) for sample SJ1.

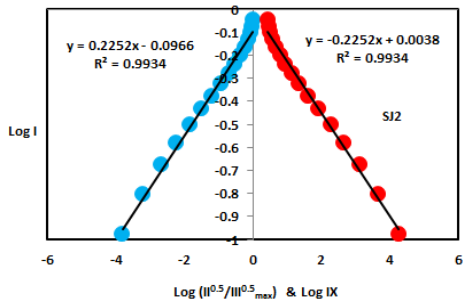

Figure 3: Log ($II^{0.5}/III_{max}^{0.5}$) versus log I (blue color)& Log IX versus log I (red color) for sample SJ2.

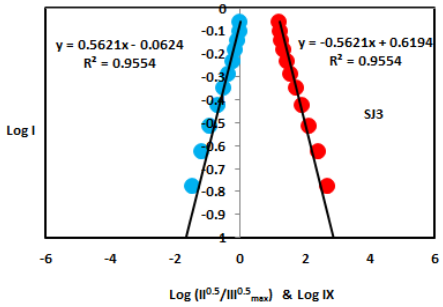

Figure 4: Log ($II^{0.5}/III_{max}^{0.5}$) versus log I (blue color)& Log IX versus log I (red color) for sample SJ3.

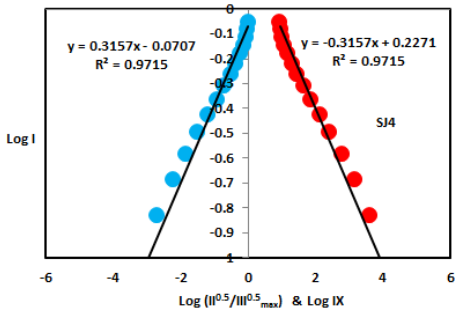

Figure 5: Log ($II^{0.5}/III_{max}^{0.5}$) versus log I (blue color) & Log IX versus log I (red color) for sample SJ4.

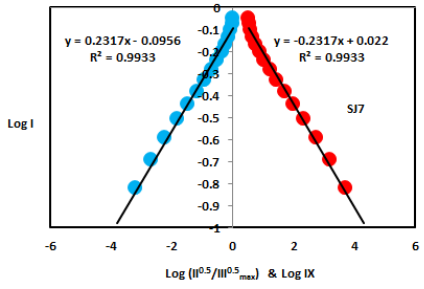

Figure 6: Log ($II^{0.5}/III_{max}^{0.5}$) versus log I (blue color)& Log IX versus log I (red color) for sample SJ7.

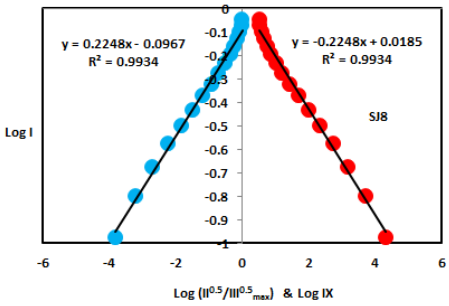

Figure 7: Log ($II^{0.5}/III_{max}^{0.5}$) versus log I (blue color)& Log IX versus log I (red color) for sample SJ8.

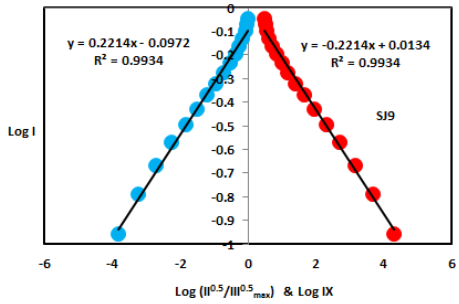

Figure 8: Log ($II^{0.5}/III_{max}^{0.5}$) versus log I (blue color)& Log IX versus log I (red color) for sample SJ9.

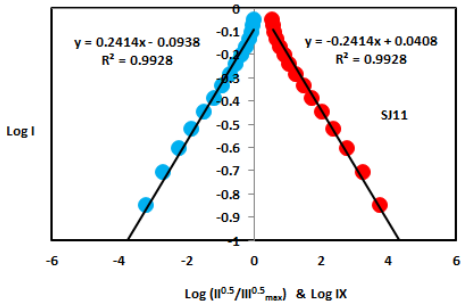

Figure 9: Log ($II^{0.5}/III_{max}^{0.5}$) versus log I (blue color)& Log IX versus log I (red color) for sample SJ11.

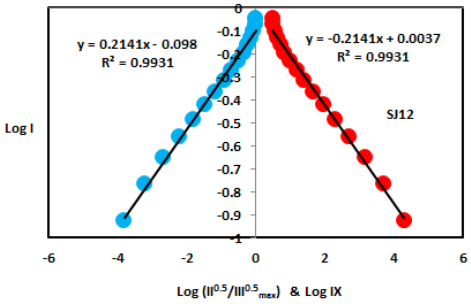

Figure 10: Log ($II^{0.5}/III_{max}^{0.5}$) versus log I (blue color)& Log IX versus log I (red color) for sample SJ12.

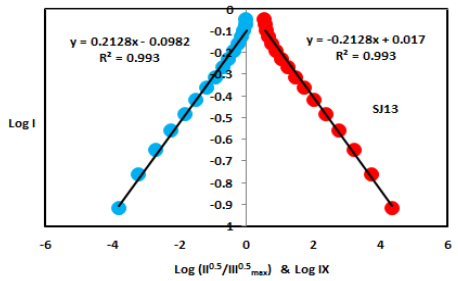

Figure 11: Log ($II^{0.5}/III_{max}^{0.5}$) versus log I (blue color)& Log IX versus log I (red color) for sample SJ13.

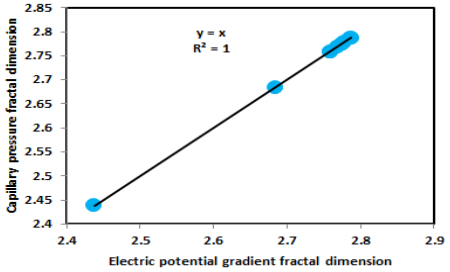

Figure 12: Electric potential gradient fractal dimension versus capillary pressure fractal dimension

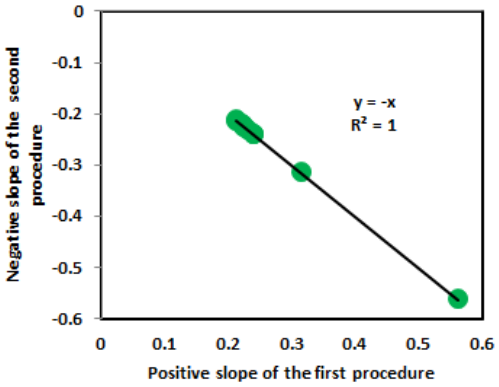

Figure 13: Positive slope of the first procedure versus negative slope of the second procedure

Formation	Reservoir	Sample	Porosity %	k (md)	Positive slope of the first procedure Slope=3-Df	Negative slope of the second procedure Slope=Df-3	Electric potential gradient fractal dimension	Capillary pressure fractal dimension
Permo-Carboniferous Shajara Formation	Upper Shajara Reservoir	SJ13	25	973	0.2128	-0.2128	2.7872	2.7872
		SJ12	28	1440	0.2141	-0.2141	2.7859	2.7859
		SJ11	36	1197	0.2414	-0.2414	2.7586	2.7586
	Middle Shajara Reservoir	SJ9	31	1394	0.2214	-0.2214	2.7786	2.7786
		SJ8	32	1344	0.2248	-0.2248	2.7752	2.7752
		SJ7	35	1472	0.2317	-0.2317	2.7683	2.7683
	Lower Shajara Reservoir	SJ4	30	176	0.3157	-0.3157	2.6843	2.6843
		SJ3	34	56	0.5621	-0.5621	2.4379	2.4379
		SJ2	35	1955	0.2252	-0.2252	2.7748	2.7748
		SJ1	29	1680	0.2141	-0.2141	2.7859	2.7859

Table 1: Petrophysical model showing the three Shajara Reservoir Units with their corresponding values of electric potential gradient fractal dimension and capillary pressure fractal dimension.

Conclusion

- The sandstones of the Shajara Reservoirs of the Shajara formation permo-Carboniferous were divided here into three units based on electric potential gradient fractal dimension
- The Units from base to top are: Lower Shajara electric potential gradient Fractal dimension Unit, Middle Shajara Electric Potential Gradient Fractal Dimension Unit, and Upper Shajara Electric Potential Gradient Fractal Dimension Unit.
- These units were also proved by capillary pressure fractal dimension.
- The fractal dimension was found to increase with increasing grain size and permeability.

Acknowledgement

The author would to thanks King Saud University, college of Engineering, Department of Petroleum and natural gas engineering, Department of Chemical Engineering, Research Centre at College of Engineering, and King Abdullah Institute for research and consulting Studies for their supports.

References

1. Toledo GT, Navy RA, Davis HT, Scriven LE (1994) Capillary pressure, water relative permeability, electrical conductivity and capillary dispersion coefficient of fractal porous media at low wetting

2. phase saturation. SPE advanced technology Series 2: 136-141.

3. Li K, Horne RN (2002) Experimental verification of methods to calculate relative permeability using capillary pressure data. SPE 76757, Proceedings of the 2002 SPE Western Region Meeting/AAPG Pacific Section Joint Meeting held in Anchorage, Alaska.

4. Li K, Willams W (2007) Determination of capillary Pressure function from resistivity data. Transp. Porous Media 67: 1-15.

5. Zhang Z, Weller A (2014) Fractal Dimension of Pore-Space Geometry of Eocene sandstone formation. Geophysics 79: D377-D387.

6. Wang Z, Pan M, Shi Y, Liu L, Xiong F, Qin Z (2018) Fractal analysis of Donghetangs and stones using NMR measurements. Energy & Fuels 32: 2973-2982.

7. Guo Y-h, Pan B-z, Zhang L-h, Fang C-h (2018) Research and application of the relationship between transverse relaxation time and resistivity index in tight sandstone reservoir. J Petrol Sci Eng 160: 597-604.

8. AlKhidir KEME (2017) Pressure head fractal dimension for characterizing Shajara Reservoirs of the Shajara Formation of the Permo-Carboniferous Unayzah Group, Saudi Arabia. Arch Pet Environ Biotechnol: 1-7.

9. Alkhidir KEME (2018) Arithmetic relaxation time of induced polarization fractal dimension for characterizing Shajara Reservoirs of the Shajara Formation. Nanosci Nanotechnol 1:1-8

10. Alkhidir KEME (2018) Geometric relaxation time of induced polarization fractal dimensionfor characterizing Shajara Reservoirs of the Shajara formation of the Permo-Carboniferous Unayzah Group-Permo. Int J Pet Res 2: 105-108.

11. Alkhidir KEME (2018) Geometric relaxation time of induced polarization fractal dimensionfor characterizing Shajara Reservoirs of The Shajara Formation of the Permo-Carboniferous Unayzah Group, Saudi Arabia. SF J Petroleum 2: 1-6.

12. AlKhidir KEME (2018) Seismo Electric field fractal dimension for characterizing Shajara Reservoirs of the Permo-Carboniferous Shajara Formation, Saudi Arabia. Pet Petro Chem Eng J 2: 1-8.

13. Alkhidir KEME (2018) Resistivity Fractal Dimension for Characterizing Shajara Reservoirs of the Permo Carboniferous Shajara Formation Saudi Arabia. Recent Adv. Petrochem Sci 5: 1-6.